



# Urea thermolysis studied under flow reactor conditions using DSC and FT-IR

Andreas Lundström, Bengt Andersson, Louise Olsson\*

Department of Chemical and Biological Engineering/Competence Centre for Catalysis, Chalmers University of Technology, SE-41296 Göteborg, Sweden

## ARTICLE INFO

### Article history:

Received 20 December 2008

Received in revised form 19 March 2009

Accepted 24 March 2009

### Keywords:

Urea decomposition

DSC

Calorimeter

FT-IR

NH<sub>3</sub>

HNCO

CYA

Biuret

Mass-transfer

Heat transfer

## ABSTRACT

The thermal decomposition of urea has been studied under flow reactor conditions using a differential scanning calorimeter (DSC) and Fourier transformed infrared spectroscopy (FT-IR). Samples of urea were administered using either a cordierite monolith impregnated with a urea/water solution or a silica cup with a dry urea sample. The samples were heated between 25 and 700 °C with heating rates of 10 and 20 K/min and the thermal response of the sample and off gas concentrations of ammonia and isocyanic acid were recorded. Biuret and cyanuric acid were decomposed in a separate set of experiments to verify some of the features observed in gas phase data during urea decomposition.

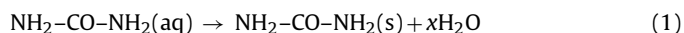
Results show that depending on the way the sample is administered, i.e. cup or monolith different behavior in the evolved gases are observed. This is due to different reactions taking place in the vessel induced by the different conditions under which the pyrolysis of urea is preformed.

© 2009 Elsevier B.V. All rights reserved.

## 1. Introduction

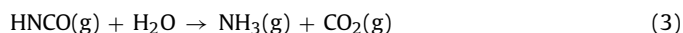
Up to date numerous studies on the thermolysis of urea have been undertaken. One of the main driving force of these studies being the introduction and commercialization of the selective catalytic reduction (SCR) catalyst for mobile heavy duty diesel applications [1–3]. For mobile applications urea is favored as it is a non-volatile source of ammonia for the selective reduction of nitrogen oxides [3–8]. Several different approaches of urea administration exist for this type of application, the most common being the direct injection of a 32.5% solution of water and urea (AdBlue) in to the exhaust stream, upstream of the catalyst.

AdBlue is believed to decompose in two steps, first water evaporates and due to the low vapor pressure of urea solid urea is formed according to reaction (1). After the water has evaporated solid urea melts and decomposes into gas phase ammonia and isocyanic acid in equimolar amounts [3,4,7,9–12].



Isocyanic acid may further react with gas phase water on the SCR-catalyst forming ammonia and carbon dioxide [3–5,7,13] via

hydrolysis according to the following reaction:



Several authors [7,9,12–14] have reported the formation of high molecular compounds such as cyanuric acid (CYA), ammeline and ammeline during urea thermolysis. In both [13] and [9,12] urea was decomposed in an open vessel type reactor using a solid urea sample.

So far only a few studies have focused on obtaining experimental data for kinetic studies of urea decomposition. Yim et al. [15] preformed flow reactor studies of urea decomposition and SCR performance using an atomizer to disperse urea in to the reaction gas. During the course of their experiments a mass balance (based on nitrogen) larger than 90% was always maintained leading to the conclusion that the formation of CYA and other high molecular compounds was negligible under their experimental conditions. Conversion of urea was found to be independent of the feed gas concentration of urea into the reactor. Birkhold et al. [16,17] used computational fluid dynamics (CFD) simulations of a complete spray of urea water solution and compared rates of urea decomposition with data from Kim et al. [18]. In their study it is concluded that the rate at which urea decomposes is lower than the water evaporation from the injected droplets.

However, since urea decomposition is strongly dependant on the conditions under which the thermolysis is performed experiments that are able to identify these conditions were set up. One aim of this work is to present a good methodology for measure-

\* Corresponding author. Tel.: +46 31 772 43 90; fax: +46 31 772 30 35.  
E-mail address: [louise.olsson@chalmers.se](mailto:louise.olsson@chalmers.se) (L. Olsson).

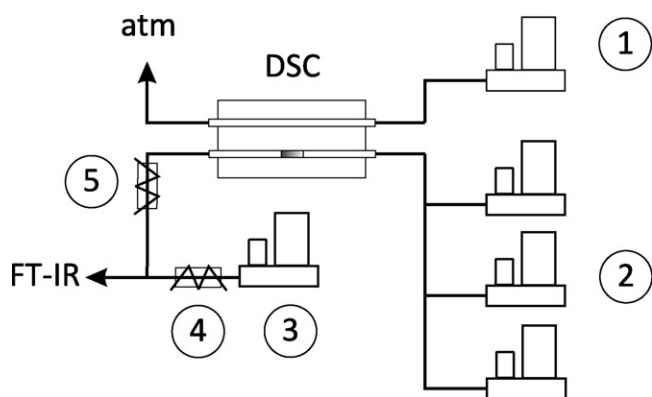


**Fig. 1.** Schematic of the experimental setup. (1) MFC for reference cell. (2) MFC for sample cell. (3) MFC for dilution to FT-IR. (4) Heating of dilution gas before FT-IR. (5) Heating of sample off gases.

ments of urea thermolysis under both flow reactor and open vessel type conditions using the same reactor set up with the aim to produce quality data for modeling of the decomposition of urea, as well as to investigate potential differences arising from the different reactor conditions. This is accomplished using both differential scanning calorimetry (DSC) and evolved gas phase analysis, i.e. FT-IR. In order to reproduce the above stated conditions, i.e. atomizer and open vessel conditions different administration strategies of the urea samples are used and compared. To imitate the atomizer a cordierite monolith impregnated with a 32.5% solution of urea and water is used. The choice of using a monolith is motivated by its favorable mass and heat transfer characteristics. In order to achieve more open vessel like conditions a silica cup is used as a method of sample delivery.

## 2. Experimental

The experimental setup is shown in Fig. 1 and consisted of mass flow controllers (MFC) to control the amount of gas going to the DSC reference and sample cells, the main DSC oven, heaters and an FT-IR for gas phase analysis.

The calorimeter used in the experiments was a Setaram Sensys DSC which also served as the reactor part of the setup. Since  $\text{NH}_3$  was expected to be one of the major products of urea thermolysis the DSC was lined with quartz-glass tubes with a outer diameter equal to 7 mm and a length of 133 mm. Due to the construction of the DSC, with a water cooling jacket at the outlet, a tube made of stainless steel heated from the outside of the calorimeter was inserted to bypass the cooling jacket. This was made in order to prevent re-condensation of isocyanic acid that would otherwise occur. The heating tube was heated to approximately  $150^\circ\text{C}$ . Two separate MFC-lines were used to supply the calorimeter, one to the calorimeters reference cell and one to the sample. This configuration gave better reproducibility compared to a simple T-junction divider. Evolved off gases were monitored using a MKS MultGas FT-IR.

The calorimeter was able to operate in two modes either vertical or horizontal depending on how the urea sample was administered to the oven. Two different ways of administering the urea sample was used; either a small cordierite monolith impregnated with a 32.5% urea solution in horizontal mode or a vertically suspended silica cup with a solid urea sample.

### 2.1. Monolith

A small 2 by 2 channel cordierite monolith with a length of 11 mm and channel width of 1 mm was used. The monolith was

impregnated with a 32.5% urea/water solution and placed in the sample cells measurement area in the horizontal position. Preparation of the solution consisted of dissolving urea with a purity greater than 99.5% (ReagentPlus Sigma–Aldrich) in ultra pure water to the desired mass fraction. The monolith was submerged in the solution for a duration of 10 min and then flushed under  $\text{N}_2$  for approximately 5 s to remove excess solution from the monolith channels. In order to determine sample loading the monolith was weighed before and after impregnation. The same monolith was used under the course of all the experiments of this type. During all monolith experiments three replicate experiments for every experimental condition were performed. In the following figures and tables these replicates will be referred to as a, b and c.

Thermolysis of biuret was performed to investigate the existence of a shoulder visible for the higher heating rate during urea thermolysis. Biuret with a purity greater than 98.5% (Fluka Analytical) was decomposed using a small cordierite plate to deliver the sample.

Two different heating rates were used during the experiments employing the monolith, 10 and 20 K/min, respectively with a temperature range of  $25\text{--}760^\circ\text{C}$ . A  $\text{N}_2$  flow of  $100\text{ ml}_n/\text{min}$  was used as a sweep gas over the sample cell. The sweep gas flow was then diluted downstream of the DSC with a flow of  $300\text{ ml}_n/\text{min}$   $\text{N}_2$  to achieve a reasonable retention time for gas phase analysis. In the reference cell a flow of  $40\text{ ml}_n/\text{min}$   $\text{N}_2$  was used, this discrepancy of non-matching flows between sample and reference being compensated for by the subtraction of a background done over an empty (not impregnated) monolith.

### 2.2. Cup

To be able to compare the experiments performed with the monolith to more open vessel/DSC type measurements experiments using a vertically suspended silica cup with a length of 11 mm, outer diameter of 3.5 mm and wall thickness of 0.5 mm were performed. The same flow conditions as in the experiments using a monolith were used but only 20 K/min heating rates were done. The cup was loaded with small granular pellets of solid urea with an approximate size of 1 mm. Background DSC runs were performed using an empty silica cup and the same cup was used in all experiments. Replicates of the cup experiments are labeled as a and b in all figures and tables referring to these experiments. Further, cyanuric acid (CYA) was decomposed using the cup as delivery vessel. The CYA used had a purity greater than 98% (Merck synthesis grade).

### 2.3. Measurements

The  $\text{NH}_3$  signal from the MKS FT-IR was calibrated against known concentrations using a 4%  $\text{NH}_3$  in Ar calibration gas with a relative tolerance of 2% in order to achieve as quantitative measurements as possible. Unfortunately calibration gas for HNCO was not available and the calibration supplied by MKS seemed to overestimate the HNCO signal. In order to make a more accurate analysis of the amount of released HNCO a calibration procedure for HNCO was developed. The method consisted of decomposing urea, in a set of independent experiments, into  $\text{NH}_3$  and HNCO. Using an accurate  $\text{NH}_3$  calibration, attained at 10 steady state points in the range 1200–10 ppm, a third order polynomial of the same form was adapted for the HNCO signal to yield the same peak area of the FT-IR signals for  $\text{NH}_3$  and HNCO during urea decomposition in these experiments. The experiments were performed using a monolith impregnated with a water/urea solution at varying concentrations and a heating rate of 10 K/min, taking special care so that no disproportion of  $\text{NH}_3$  and HNCO would be possible. The integrated peak areas of the calibrated  $\text{NH}_3$  signal and the raw HNCO signal exhibited a high degree of linearity with almost zero offset and hence the adopted polynomial was used to adjust the HNCO signal.

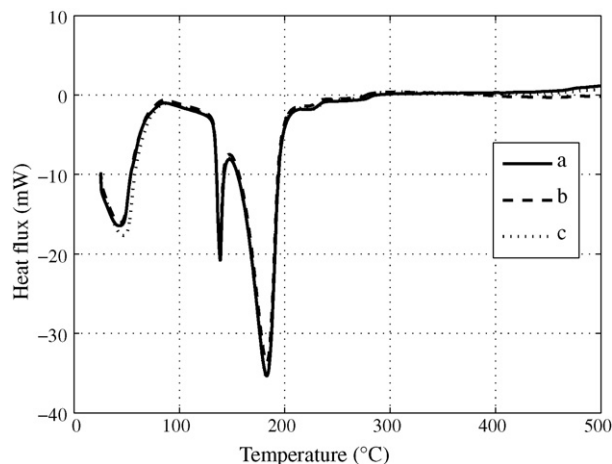


**Fig. 2.** Three DSC curves a, b and c of a 32.5% urea/water solution under a 100 ml<sub>n</sub>/min N<sub>2</sub> sweep flow and a heating rate of 10 K/min. The samples were administered using a cordierite monolith.

All calorimetric data was attained using an empty reference cell and the obtained data then subsequently adjusted by subtracting a background. The background calorimetric runs were performed using the empty sample holder, i.e. monolith or cup under the same conditions used in the original experiment.

### 3. Results and discussion

#### 3.1. Monolith 10 K/min

The DSC curve for a 32.5% urea and water sample during an experiment using a monolith is presented in Fig. 2. The experiment was performed using a heating rate of 10 K/min with a temperature range from 25 to 750 °C. Produced off gases, i.e. NH<sub>3</sub> and HNCO are shown in Figs. 3 and 4, respectively. In the DSC curve three distinct thermal events are visible, the evaporation of water from the sample at approximately 25 < T < 90 °C, melting of urea 133 °C and decomposition of urea 150 < T < 210 °C. During the decomposition phase NH<sub>3</sub> and HNCO are the main decomposition products observed in the gas phase as seen in Figs. 3 and 4. Table 1 summarizes the amount of recovered NH<sub>3</sub> and HNCO from the gas phase.

The mass balance for NH<sub>3</sub> and HNCO are presented in Table 1. The mass balance for NH<sub>3</sub> is in good agreement with the amount

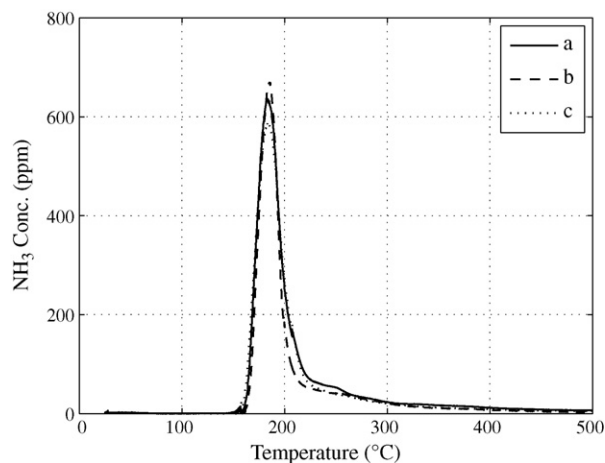


**Fig. 3.** NH<sub>3</sub> production from three experiments a, b and c of a 32.5% urea/water solution under a 100 ml<sub>n</sub>/min N<sub>2</sub> sweep flow and a heating rate of 10 K/min. The sample was administered using a cordierite monolith.

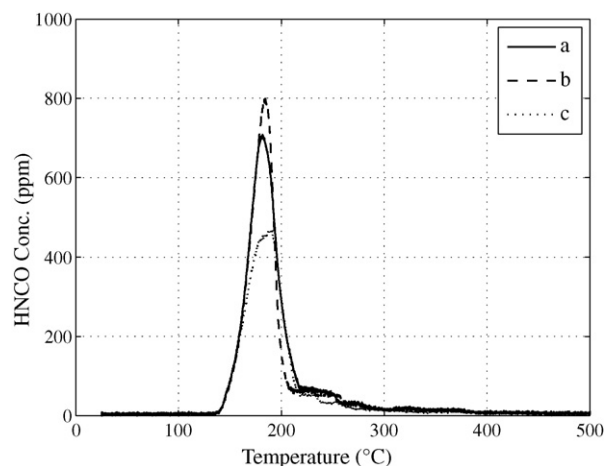


**Fig. 4.** HNCO production from three experiments a, b and c of a 32.5% urea/water solution under a 100 ml<sub>n</sub>/min N<sub>2</sub> sweep flow and a heating rate of 10 K/min. The sample was administered using a cordierite monolith.

**Table 1**

Total recovered amounts of NH<sub>3</sub> and HNCO based on charged urea. Experimental conditions were 25–750 °C 10 K/min under 100 ml<sub>n</sub>/min N<sub>2</sub> using a monolith saturated with a 32.5% urea/water solution.

Experiment 10 K/min	Urea loading (mg)	NH <sub>3</sub> recovered	HNCO recovered
a	2.76	91%	104%
b	2.70	83%	101%
c	2.73	87%	81%

of charged urea (83–91%). However, the amount of HNCO is slightly over predicted compared to the NH<sub>3</sub> signal. The NH<sub>3</sub> signal was calibrated before each run and the HNCO signal calibrated as described earlier. Good mass balances of NH<sub>3</sub> are obtained and the HNCO signal seems to follow the same trend except for a discrepancy in experiment (c) where the HNCO signal seems under predicted as compared to experiments (a) and (b). This was probably due to a malfunction of the heated tube used to bypass the DSC's cooling jacket, which lead to condensation of HNCO and consequently a deficit in the mass balance.

#### 3.2. Monolith 20 K/min

Also experiments under the same conditions as above but with a heating rate of 20 K/min were preformed. The DSC curve shown in Fig. 5 shows the same trends as that of the 10 K/min experiment but with peaks shifted towards higher temperatures due to the slower heat flux at this heating rate, i.e. 20 K/min. However, compared to the 10 K/min experiments the mass balances for the 20 K/min experiments presented in Table 2 show better concurrency. This was the reason that only heating rates of 20 K/min were considered for the cup experiments. Both curves of evolved NH<sub>3</sub> and HNCO presented in Figs. 6 and 7 show evidence of a small shoulder after their initial maxima. The existence of a shoulder at 190 °C < T < 300 during gas phase evolution could be an indication of a separate process for NH<sub>3</sub> and HNCO release overlapping with that of the main path

**Table 2**

Total recovered amounts of NH<sub>3</sub> and HNCO based on charged urea. Experimental conditions were 25–750 °C, 20 K/min under 100 ml<sub>n</sub>/min N<sub>2</sub> using a monolith saturated with a 32.5% urea/water solution.

Experiment 20 K/min	Urea loading (mg)	NH <sub>3</sub>	HNCO
a	2.6	99%	110%
b	2.67	104%	114%
c	2.76	100%	111%

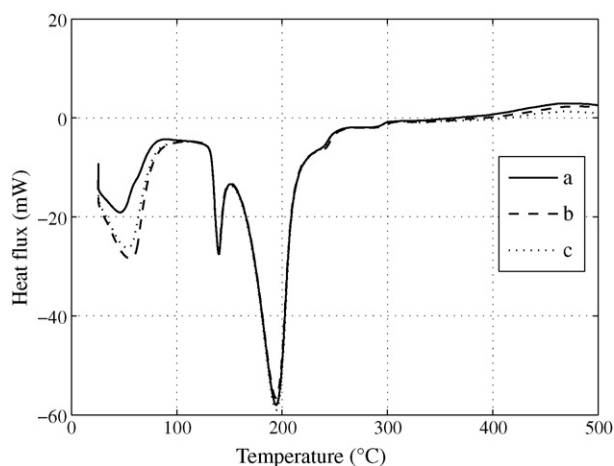


**Fig. 5.** Three DSC curves a, b and c of a 32.5% urea/water solution under a  $100 \text{ ml}_n/\text{min}$   $\text{N}_2$  sweep flow and a heating rate of  $20 \text{ K}/\text{min}$ . The samples were administered using a cordierite monolith.

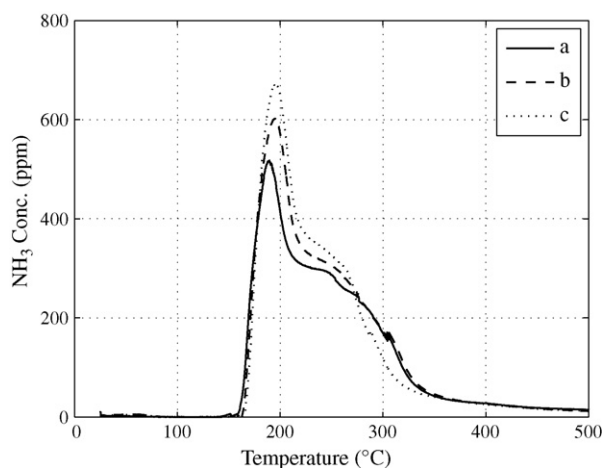


**Fig. 6.**  $\text{NH}_3$  production from three experiments a, b and c of a 32.5% urea/water solution under a  $100 \text{ ml}_n/\text{min}$   $\text{N}_2$  sweep flow and a heating rate of  $20 \text{ K}/\text{min}$ . The sample was administered using a cordierite monolith.

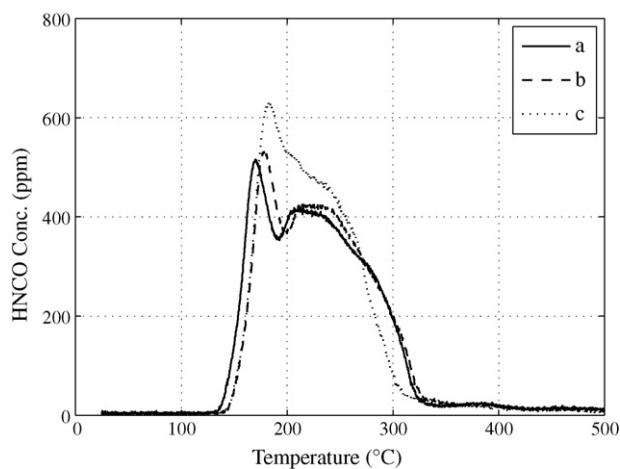


**Fig. 7.** HNCO production from three experiments a, b and c of a 32.5% urea/water solution under a  $100 \text{ ml}_n/\text{min}$   $\text{N}_2$  sweep flow and a heating rate of  $20 \text{ K}/\text{min}$ . The sample was administered using a cordierite monolith.

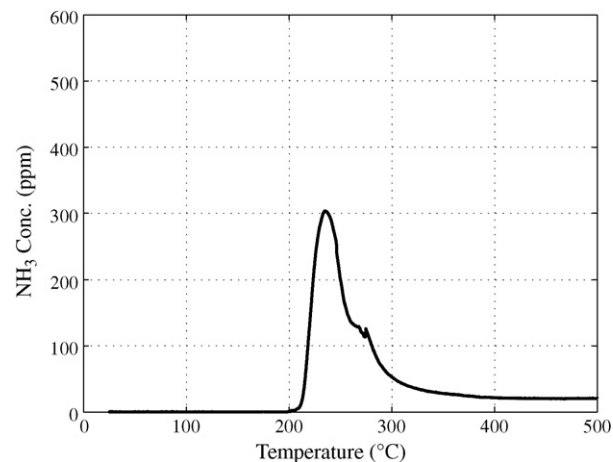


**Fig. 8.**  $\text{NH}_3$  production during decomposition of biuret under a  $100 \text{ ml}_n/\text{min}$   $\text{N}_2$  sweep flow and a heating rate of  $20 \text{ K}/\text{min}$ . The sample was administered using a plate made of cordierite.

of urea thermolysis, i.e. Eq. (2). Further, the shoulder seems to be more pronounced for the HNCO signal than for  $\text{NH}_3$ . This will be discussed in more detail below.

### 3.3. Biuret decomposition $20 \text{ K}/\text{min}$

A separate study of biuret decomposition was performed to investigate the development of the shoulder visible in the  $20 \text{ K}/\text{min}$  monolith experiments. The evolution of  $\text{NH}_3$  and HNCO are presented in Figs. 8 and 9. As biuret decomposes two distinct features in evolved gases are visible. Decomposition starts around  $200^\circ\text{C}$  and up to  $250^\circ\text{C}$  more  $\text{NH}_3$  than HNCO is evolved. After  $250^\circ\text{C}$  the situation is reversed and a sharp increase of evolved HNCO is noted. This may be explained by the formation of CYA during decomposition of biuret where CYA may be formed either via direct polymerization of HNCO or the reaction between biuret and HNCO. Thus the sharp increase in evolved HNCO observed above  $250^\circ\text{C}$  is probably due to CYA decomposition according to reaction (8). This observation is also in accordance with Schaber et al. [9] who also observed CYA formation during biuret decomposition. In the  $20 \text{ K}/\text{min}$  monolith experiments (Figs. 6 and 7) the shoulder of HNCO and  $\text{NH}_3$  occurs between  $200$  and  $300^\circ\text{C}$ , with a maximum at  $250^\circ\text{C}$ , which coincides perfectly with the decomposition temperature of biuret.

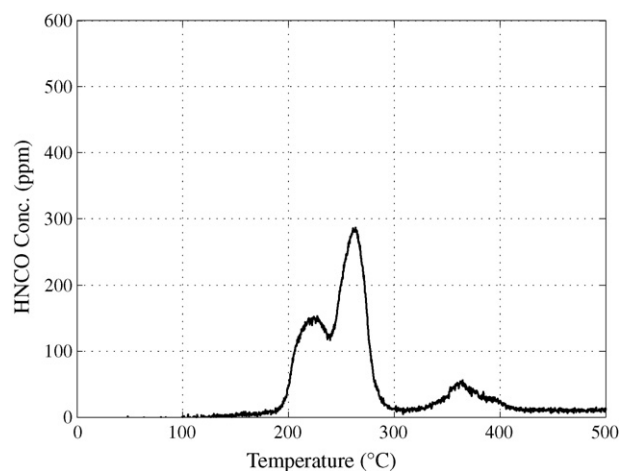


**Fig. 9.** HNCO production during decomposition of biuret under a  $100 \text{ ml}_n/\text{min}$   $\text{N}_2$  sweep flow and a heating rate of  $20 \text{ K}/\text{min}$ . The sample was administered using a plate made of cordierite.

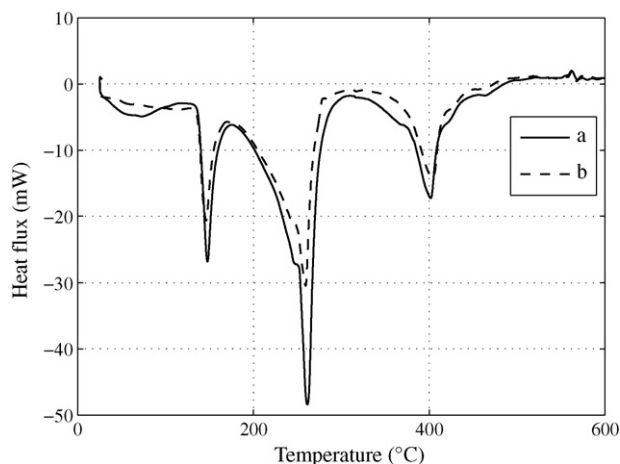


**Fig. 10.** Two DSC curves a and b for a solid urea sample under a 100 ml<sub>n</sub>/min N<sub>2</sub> sweep flow and a heating rate of 20 K/min. The samples were administered using a silica cup.

These results show that the shoulder visible in the 20 K/min monolith experiments is likely due to the formation and subsequent decomposition of biuret during urea thermolysis.

### 3.4. Cup 20 K/min

DSC results for the cup experiments are presented in Fig. 10 and show one new large feature above 300 °C compared to the monolith experiments. This peak seems to correlate to a second release of HNCO but not NH<sub>3</sub>, as seen in Figs. 11 and 12. The recovery of NH<sub>3</sub> is above 90% for both repeated experiments, but HNCO recovery is only about 27% in the first peak. In the second HNCO peak an additional 24% (based on initial urea loading) of HNCO is observed. This implies that the formed by-product decomposes to HNCO in the gas phase and that the conditions under which urea thermolysis is performed, i.e. cup or monolith, is important for the overall distribution of formed products. Further, the peaks in gas phase data and thermal response are shifted towards even higher temperatures than compared to the monolith experiments. This is due to the slower heat transfer to the cup as compared to the monolith, thus illustrating one of the benefits of using a monolith.

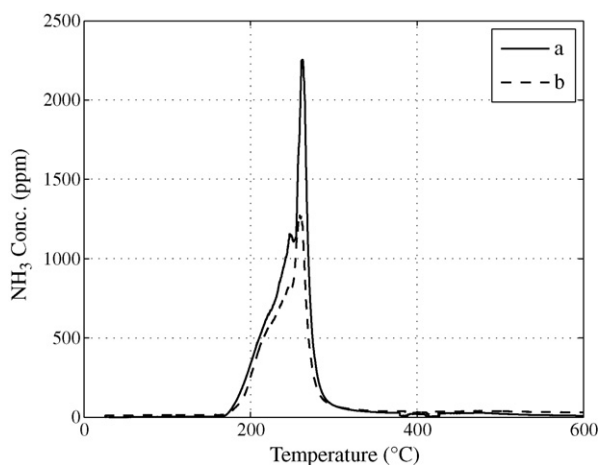


**Fig. 11.** NH<sub>3</sub> production from two experiments a and b for a solid urea sample under a 100 ml<sub>n</sub>/min N<sub>2</sub> sweep flow and a heating rate of 20 K/min. The sample was administered using a silica cup.

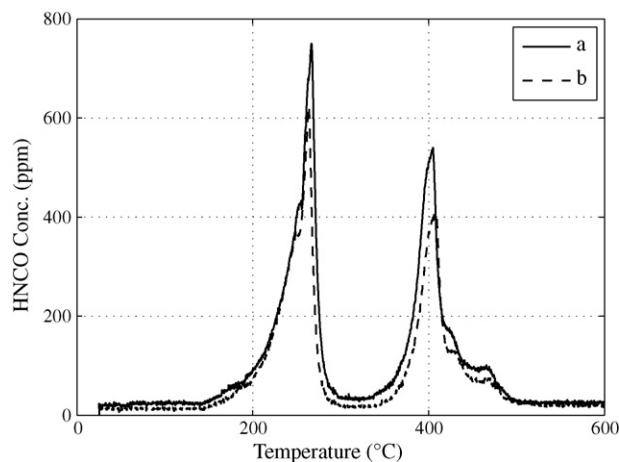


**Fig. 12.** HNCO production from two experiments a and b for a solid urea sample under a 100 ml<sub>n</sub>/min N<sub>2</sub> sweep flow and a heating rate of 20 K/min. The sample was administered using a silica cup.

### 3.5. CYA decomposition 20 K/min

To verify the secondary release of HNCO in the 20 K/min cup experiments CYA was decomposed using the silica cup. The results presented in Figs. 13 and 14 show that CYA starts to decompose at 400 °C, with a maximum peak at 440 °C in the cup experiments. The second peak in the urea decomposition experiment using a cup was observed at about 400 °C, which correlates very well to the decomposition temperature of CYA. We therefore suggest that the decomposition of urea in the cup experiments results in a high temperature HNCO peak due to decomposition of CYA.

Several reports of biuret formation during urea thermolysis have been presented [9,12–14]. Schaber et al. [9,12] reports the formation of biuret under open vessel conditions. They suggest that biuret is formed at approximately 160 °C by the reaction between unreacted urea and gas phase HNCO according to reaction (4). At temperatures above 190 °C (the melting point of biuret) biuret is reported to decompose back into urea and HNCO, i.e. the reverse of reaction (4). This is supported in our data by the existence of a shoulder in evolved gas phase NH<sub>3</sub> and HNCO for the 20 K/min monolith experiments, i.e. Figs. 6 and 7. Moreover, the fact that the shoulder is more pronounced for HNCO seems reasonable since HNCO would then be formed both directly via decomposition of biuret and via the released urea whereas NH<sub>3</sub> would only be formed via decomposing

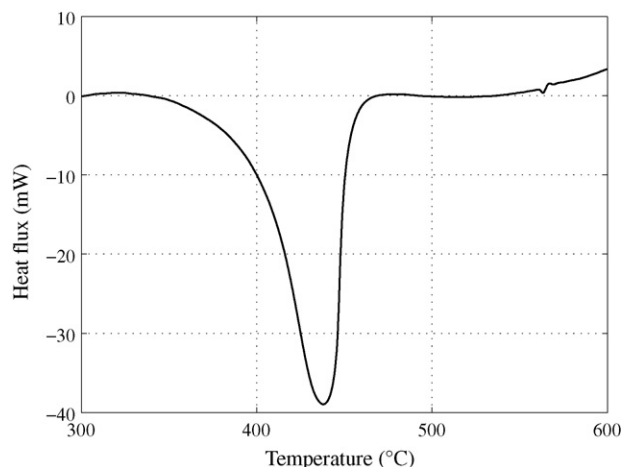


**Fig. 13.** DSC curve for a solid CYA sample under a 100 ml<sub>n</sub>/min N<sub>2</sub> sweep flow and a heating rate of 20 K/min. The sample was administered using a silica cup.

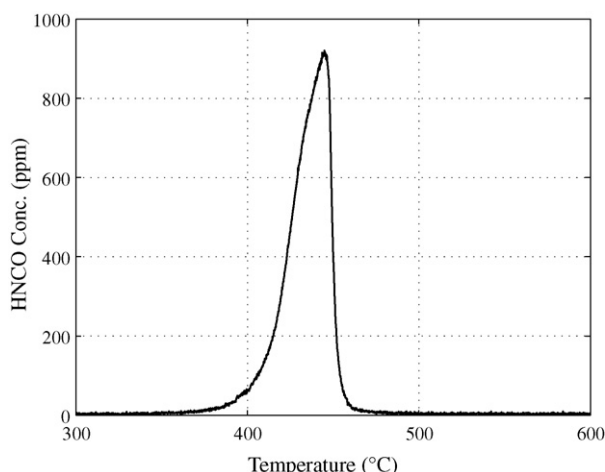
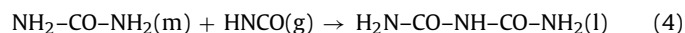


**Fig. 14.** HCNCO production from a solid CYA sample under a 100 ml<sub>n</sub>/min N<sub>2</sub> sweep flow and a heating rate of 20 K/min. The sample was administered using a silica cup.

urea. The experiments using pure biuret under the same reaction conditions supports this conclusion and further implies that CYA may form during biuret decomposition. In the 10 K/min monolith and 20 K/min cup experiments the shoulder is no longer noticeable. It has been concluded by Fang and Dacosta [13] that the relative abundance of formed biuret depends on the heating rate. This is most probably due to the different efflux rates of HCNCO, depending on the chosen heating rate, which would result in different average gas phase concentrations for the same residence time in the monolith experiments. This is also observed in the experiments, where the 10 K/min monolith experiments give HCNCO gas phase concentrations of about 500 ppm in the peak, but the 20 K/min gives as much as 700–800 ppm HCNCO. We suggest that the higher concentration of HCNCO in the 20 K/min experiment is the reason for the biuret formation and the absence of a shoulder in evolved NH<sub>3</sub> and HCNCO for the 10 K/min experiment is due to the lower gas phase concentrations of HCNCO. For the 20 K/min cup experiments the much lower evolution of HCNCO compared to NH<sub>3</sub> during the initial decomposition suggests that HCNCO is being consumed and in combination with the lack of a shoulder could be indicative of released HCNCO only being active in the formation of CYA under these conditions. Further, high formation rates of CYA are expected in the cup experiments where the overall gas phase concentrations of HCNCO are high due to the lower mass transfer rates out from the cup to the surrounding bulk gas (sweep gas) as compared to the monolith experiments.



Further, biuret is suggested to work as an intermediate to form CYA [9,12–14]. Either via the continued reaction of gas phase HCNCO with formed biuret according to reaction (5) as suggested by Schaber et al. [9,12] or as proposed by Fang and Dacosta [13] by reaction of intact urea and biuret reaction (6).

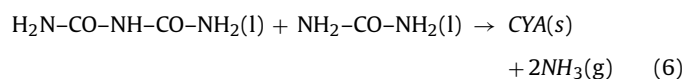


**Table 3**

Total recovered amounts of NH<sub>3</sub> and HCNCO based on charged urea. Experimental conditions were 25–750 °C 20 K/min under 100 ml<sub>n</sub>/min N<sub>2</sub> using a cup with solid urea pellets. (i) Recovered amount of HCNCO in first peak and (ii) recovered amount of HCNCO in the second peak.

Experiment 20 K/min	Urea loading (mg)	NH <sub>3</sub>	HCNCO (i)	HCNCO (ii)	HCNCO (tot)
a	4.6	93%	27%	24%	51%
b	3.5	91%	29%	24%	53%

In both cases the net result would be the same if Eq. (6) is considered to be the overall observed reaction of decomposed urea and CYA formation. Even though the route for CYA formation with biuret as a precursor is considered to be the most probable [9,12], other pathways have been reported. Herzberg and Ried [19] have reported the direct polymerization of gas phase HCNCO to CYA if a critical vapor pressure is exceeded Eq. (7).

Our data shows a large thermal event in the temperature interval 320 < T < 450 °C in the cup experiments. This may be attributed to sublimation and decomposition of formed CYA which has been reported by Stradella and Argentero [14] to sublimate and decompose at approximately 350 < T < 400 °C and by Schaber et al. [9,12] at approximately 275 < T < 375 °C. Fang and Dacosta [13] found that one of main products after the first decomposition stage of urea was CYA. In their study Schaber et al. [9,12] suggest that the main mechanism for CYA decomposition is the direct decomposition into HCNCO according to Eq. (8). Even though the decomposition of CYA proceeds rather slowly at these modest temperatures several authors support the fact that CYA sublimates and decomposes with a loss of HCNCO to the gas phase [20,21].



Data presented in Table 3 seems to agree with the fact that in all the proposed mechanisms the net evolved NH<sub>3</sub> during the main part of decomposition, i.e. 170 < T < 280 °C is unchanged (compared to the experiments performed with a monolith). The absence of a shoulder in the cup experiments is not conclusive enough to distinguish which mechanism is important for CYA formation, i.e. via reaction between HCNCO and biuret or direct polymerization.

Schaber et al. [9,12] observed the formation of ammelide which was also attributed to using biuret as a precursor in its formation. Even though, ammelide was reported to decompose in approximately the same temperature range as CYA much less was formed.

#### 4. Conclusions

The mechanisms for urea thermolysis are strongly dependant on the conditions under which the experiments are performed. Using either an impregnated monolith or cup produces very different responses in both evolved gas phase species and thermal response. For the cup experiments higher gas phase concentrations of reactants are expected due to lower mass transfer rates as compared to the monolith. Also different heating rates play an important role for the distribution of possible by-products during urea thermolysis. This is attributed to the corresponding variation in efflux rates of the different reactants, e.g. a higher heating rate will lead to higher gas phase concentration of possible reactants. This is clearly seen in the case of using a monolith where a higher heating rate leads to the formation of biuret. We further suggest in agreement with previous studies that CYA is formed as a by-product in the cup experiments. This is due to high local concentrations of HCNCO and the direct polymerization of HCNCO is under the current conditions, i.e. cup the most probable pathway to CYA. These results are supported by experiments for decomposition of CYA, which occurs at the same temperature interval.

Further, good flow reactor experiments of urea thermolysis using a cordierite monolith impregnated with a urea/water solu-

tion is possible and the quality is sufficient for kinetic modeling. The advantages of using a monolith being the very good mass and heat transfer characteristics. Contrasting the monolith experiments to the cup experiments opens up for the possibility to isolate different processes, such as CYA and biuret formation, induced by the very different conditions prevailing in each delivery strategy.

### Acknowledgements

This work has been performed within the Competence Centre for Catalysis, which is financially supported by Chalmers University of Technology, the Swedish Energy Agency and the member companies: AB Volvo, Volvo Car Corporation, Scania CV AB, GM Powertrain Sweden AB, Haldor Topsoe A/S and The Swedish Space Agency. One author (Louise Olsson) would also like to acknowledge the Swedish Research Council (contract: 621-2003-4149 and 621-2006-3706) for additional support. The financial support for the micro calorimeter from the Swedish Research Council (contract: 621-2003-4149 and 621-2006-3706) and for the FT-IR from Knut and Alice Wallenberg Foundation, Dnr KAW 2005.0055, is gratefully acknowledged.

### References

- [1] M. Koebel, M. Elsener, G. Madia, Reaction pathways in the selective catalytic reduction process with NO and NO<sub>2</sub> at low temperatures, *Ind. Eng. Chem. Res.* 40 (2001) 52–59.
- [2] M. Koebel, M. Elsener, G. Madia, Recent advances in the development of urea-SCR for automotive applications, *SAE Technical Paper Series* 2001-01-3625, 2001.
- [3] C.S. Sluder, J.M.E. Storey, S.A. Lewis, L.A. Lewis, Low temperature urea decomposition and SCR performance, *SAE Technical Paper Series* 2005-01-1858, 2005.
- [4] M. Koebel, M. Elsener, M. Kleemann, Urea-SCR: a promising technique to reduce NOx emissions from automotive diesel engines, *Catal. Today* 59 (2000) 335–345.
- [5] G. Madia, M. Koebel, M. Elsener, A. Wokaun, Side reactions in the selective catalytic reduction of NOx with various NO<sub>2</sub> fractions, *Ind. Eng. Chem. Res.* 41 (2002) 4008–4015.
- [6] E. Seker, N. Yasyerli, E. Gulari, C. Lambert, R.H. Hammerle, NOx reduction by urea under lean conditions over single step sol-gel Pt/alumina catalyst, *Appl. Catal. B* 37 (2002) 27–35.
- [7] M. Koebel, E.O. Strutz, Thermal and hydrolytic decomposition of urea for automotive selective catalytic reduction systems: thermochemical and practical aspects, *Ind. Eng. Chem. Res.* 42 (2003) 2093–2100.
- [8] Y. Park, J.A. Caton, A study of urea decomposition and a comparison between urea and ammonia as NOx reducing agents, in: *Regional Proceedings ASME International Southwest Region X Thecnocal Conference*, March 28–29, 2009, Houston, TX, 2009.
- [9] P.M. Schaber, J. Colson, S. Higgins, D. Thielen, B. Anspach, J. Brauer, Thermal decomposition (pyrolysis) of urea in an open reaction vessel, *Thermochim. Acta* 424 (2004) 131–142.
- [10] M. Kleemann, M. Elsener, M. Koebel, A. Wokaun, Hydrolysis of isocyanic acid on SCR catalysts, *Ind. Eng. Chem. Res.* 39 (2000) 4120–4126.
- [11] M.U. Alzueta, R. Bilbao, A. Millera, M. Oliva, J.C. Ibañez, Interactions between nitric oxide and urea under flow reactor conditions, *Energy Fuels* 12 (1998) 1001–1007.
- [12] P.M. Schaber, J. Colson, S. Higgins, E. Dietz, D. Thielen, B. Anspach, J. Brauer, *Am. Lab.* 31 (1999) 13–21.
- [13] H.L. Fang, H.F.M. DaCosta, Urea thermolysis and NOx reduction with and without SCR catalysts, *Appl. Catal. B* 46 (2003) 17–34.
- [14] L. Stradella, M. Argentero, A study of the thermal decomposition of urea, of related compounds and thiourea using DSC and TG-EGA, *Thermochim. Acta* 219 (1993) 315–323.
- [15] S.D. Yim, S.J. Kim, J.H. Baik, I.-S. Nam, Decomposition of urea into NH<sub>3</sub> for the SCR process, *Ind. Eng. Chem. Res.* 43 (2004) 4856–4863.
- [16] F. Birkhold, U. Meingast, P. Wassermann, O. Deuschmann, Modeling and simulation of the injection of urea-water-solution for automotive SCR DeNOx-systems, *Appl. Catal. B: Environ.* 70 (2007) 119–127.
- [17] F. Birkhold, U. Meingast, P. Wassermann, O. Deuschmann, Analysis of the injection of urea-water-solution for automotive SC DeNOx-systems: modeling of two-phase flow and spray/wall-interaction, *SAE Technical Paper Series* 2006-010643, 2006.
- [18] J.Y. Kim, S.H. Ryu, J.S. Ha, Numerical prediction on the characteristics of spray-induced mixing and thermal decomposition of urea solution in SCR system, in: *Proceedings of the 2004 Fall Technical Conference of the ASME Internal Combustion Engine Division*, Long Beach, California, USA, 2004.
- [19] G. Herzberg, C. Reid, Infra-red spectrum and structure of the HNCO molecule, *Disc. Faraday Soc.* 9 (1950) 92–99.
- [20] J. Mercadier, M. Pignon, F. Calabuig, J. Lédé, J. Villermaux, Kinetics of isocyanuric acid pyrolysis, *J. Anal. Appl. Pyrol.* 28 (1994) 107–120.
- [21] H.G. Langer, T.P. Brady, Thermal reactions by automated mass spectrometric thermal analysis, *Thermochim. Acta* 5 (1973) 391–402.